www.czasopisma.pan.pl PAN POLSKA AKADEMIA NAUK www.journals.pan.pl

Arch. Metall. Mater. **62** (2017), 2, 581-586

DOI: 10.1515/amm-2017-0086

A. SZCZOTOK*#

METALLOGRAPHIC STUDY OF THE CASTING MADE FROM CMSX-6 SC NICKEL-BASED SUPERALLOY

Microstructural characterization is an important tool to optimize the properties of engineering materials. Quantitative metallography is a common technique, which provides three-dimensional estimations of phases and structure elements from two-dimensional images. Metallography has been described as both a science and an art [1].

Superalloys are high-performance alloys which exhibits excellent mechanical strength and creep resistance at high temperatures, good surface stability, and corrosion and oxidation resistance. Temperature and corrosion resistant materials such as nickel-based superalloys are prepared mostly with standard metallographic techniques. However, the results can be significantly improved by using finely graded CMP (chemical mechanical polish) polishing solutions on a high napped polishing pad.

Sample preparation requires a certain degree of skills and experience, due to the high chemical resistance of most superalloys. Some chemical solutions are able to dissolve the γ matrix and recover the γ' residue, and some others solutions can be used to obtain a contrary effect – dissolve the γ' phase precipitates and recover the γ matrix residue. The aim of the presented research is to describe qualitatively and quantitatively the as-cast microstructure of CMSX-6 SC superalloy. The author's attention has been concentrated on the γ' phase precipitates morphology. The results of using optical and scanning electron microscopy (SEM) are presented.

Keywords: superalloy, CMSX-6, microstructure, image analysis.

1. Introduction

Metallographic study of every investigated material requires some activities done according to a certain order. Planned earlier sequence of laboratory works makes repeatable microstructure studies of a material possible. This sequence of actions includes: a determination of the aim of the studies, an appropriate sampling strategy, selection of two- and tree-dimensional parameters describing phases or elements occurring in the material, specimen preparation, a revealing of phases or structural elements by various selective etching methods, a selection of parameters of an image acquisition of precipitations with light or scanning electron microscopy, an automatic detection of the studied precipitations using computer aided image analysis, a performance of measurements and results analysis, calculation of stereological parameters and their relative errors, a determination of minimal number of measurements, an analysis of repeatability of results, and finally a proper graphical presentation of the results. Every of the above given actions is important, many of them are indispensable and can affect the obtain results.

2. Material and method

The study presents metallographic investigations of the cast bars from CMSX-6 single crystal nickel-based superalloy. CMSX is registered trademark of the Cannon-Muskegon Corporation [2]. The nickel-based single crystal superalloy CMSX-6 has been developed by Cannon-Muskegon in conjunction with MTU for those high temperature applications where low density is a primary design requirement, as it is the case for aeroengine blades [3,4]. The typical chemical composition in weight percent of the alloys used is given in Table 1. The studied alloy is free of C and the grain boundary stabilizing element is Hf (see in Table 1). This leads to an increased melting temperature and an improved high temperature creep rupture strength [5].

TABLE 1

Typical chemical composition of the CMSX-6 SC alloy [2]

Element (wt %)													
C	**Cr**	**Ni**	**Co**	**Mo**	**W**	**Nb**	**Ta**	**Ti**	**Al**	**B**	**Zr**	**Hf**	**Re**
—	10	bal.	5	3	—	—	2	4.7	4.8	—	—	0.1	—

According to Ref. [5] for CMSX-6 it seems to be possible to produce single crystal castings with very fine and homogeneous dendritic microstructure, resulting in improved mechanical properties. The metallographic analysis performed in [5] suggests that the solidification process of the alloy CMSX-6 starts with the crystallization of the γ-phase, and is completed by the eutectic reaction L+ γ + γ'. No carbides were observed.

* SILESIAN UNIVERSITY OF TECHNOLOGY, FACULTY OF MATERIALS ENGINEERING AND METALLURGY, 8 KRASINSKIEGO STR., 40-019 KATOWICE, POLAND

Corresponding author: agnieszka.szczotok@polsl.pl

The test bars used in this study were produced in the vacuum induction melting furnace ALD for investment casting of equiaxed, directionally solidified and single crystal materials in Research and Development Laboratory for Aerospace Materials in Rzeszow. This ALD furnace has a conventional Bridgman crystal-growing method. A speed of a few inches per hour is typical.

The bar was approximately 8 mm in diameter by 205 mm long. Following casting, the bar was visually inspected, X-ray inspected and characterized using standard metallographic techniques for as cast microstructure.

The bar intended for investigations was cut perpendicularly to the main axis. The transverse cross-section from the middle part of the bar were cut off for sample preparation. The cross-section for the microstructural investigations by light microscopy (LM) and scanning electron microscopy (SEM) was included and prepared using standard metallographic mechanical grinding and polishing techniques based on the nickel-base superalloy preparation system [6]. Correctly prepared, without artefacts, metallographic specimens were intended for researches using LM and SEM. The procedure of the metallographic specimen preparation was presented in detail in Table 2. Finally, the specimens were chemically etched in 100 ml H_2O, 100 ml HCl, 100 ml HNO_3 and 3 g MoO_3.

TABLE 2

Materials and parameters of the specimen preparation

	Surface	Abrasive/size	Load (N)/ specimen	Base speed (rpm)/ direction	Time (min)
Stage 1	Carbi-met disc	P180 grit SiC, water cooled	25	350 /complementary direction (platen and specimen holder both rotate in the same direction)	Until plane surface
Stage 2	Carbi-met disc	P320 grit SiC, water cooled	25	350 /complementary direction	1÷2
Stage 3	Carbi-met disc	P600 grit SiC, water cooled	25	350 /complementary direction	1÷2
Stage 4	Ultra-Pol cloth	9-μm Metadi Supreme – diamond suspension	25	150 /opposite direction (platen and specimen holder rotate in opposite direction)	4
Stage 5	Trident cloth	1-μm Metadi Supreme – diamond suspension	20	150 /opposite direction	4
Stage 6	Chemo-met pads	Masterprep 0.05-μm alumina suspension	20	150 /opposite direction	1
Stage 7	Micro-cloth	Masterprep 0.05-μm alumina suspension	-	Vibratory polishing	3 x 60

3. Results

Within the single crystal of this superalloy, there are two phases present, a gamma (γ) matrix and an intermetallic gamma prime (γ') precipitate/dispersed in a γ matrix, as well as ($\gamma + \gamma'$) eutectic islands with the rosette structure. The γ dendrite structures are visible in the as-cast superalloy (Fig. 2). Various magnifications and image acquisition conditions were needed for the quantitative image analysis of the γ' phase precipitates and ($\gamma + \gamma'$) eutectic islands (Fig. 1).

The ($\gamma + \gamma'$) eutectic and the γ'. precipitates in the γ matrix are not visible on the unetched samples of the alloy. The images in Fig. 1 are result of etching the alloy in 100 ml H_2O, 100 ml HCl, 100 ml HNO_3 and 3 g MoO_3 solution.

The experimental results showed a significant difference in the size and morphology of the γ' precipitates at the dendrite cores, interdendritic regions and within ($\gamma + \gamma'$) eutectic islands. The mean size distribution of the γ' phase precipitates depends on the chemical homogeneity (Figs. 2 and 3).

Secondary electrons (SE) technique of SEM microscopy was applied for imaging (Fig. 4). The images were registered using scanning electron microscope FE SEM HITACHI 4200 equipped with X-ray spectrometer NORAN VOYAGER 3500.

For a quantitative evaluation of the γ' phase precipitates in the studied CMSX-6 a series of 10 images for every one of the three area types with these precipitates were registered and then evaluated by Met-Ilo program [7]. The set of transformations from initial images into binary images for a measurement performing was worked out. The morphological operations available in Met-Ilo program ensuring repeatable detection results were applied during the initial images transformations into binary images. The binary images in satisfactory way presented precipitates of the γ' phase.

The examples of a detection of differentiated morphology of γ' phase precipitates are presented in Fig. 3.

The selected morphological and stereological parameters describing γ' phase precipitates were measured and estimated. The results of the quantitative evaluation of γ' phase precipitates in particular areas of the microstructure are presented in Tables 3-5.

The total value of volume fraction was estimated on the basis of the observation and measurements of three types of the γ' phase precipitates morphology occurring at the dendritic cores, within the ($\gamma + \gamma'$) eutectic islands and at the interdendritic regions. Further we need also the results of the area of the ($\gamma + \gamma'$) eutectic islands (the example of detection using LM is presented in Fig. 4), and area of the interdendritic regions without ($\gamma + \gamma'$)

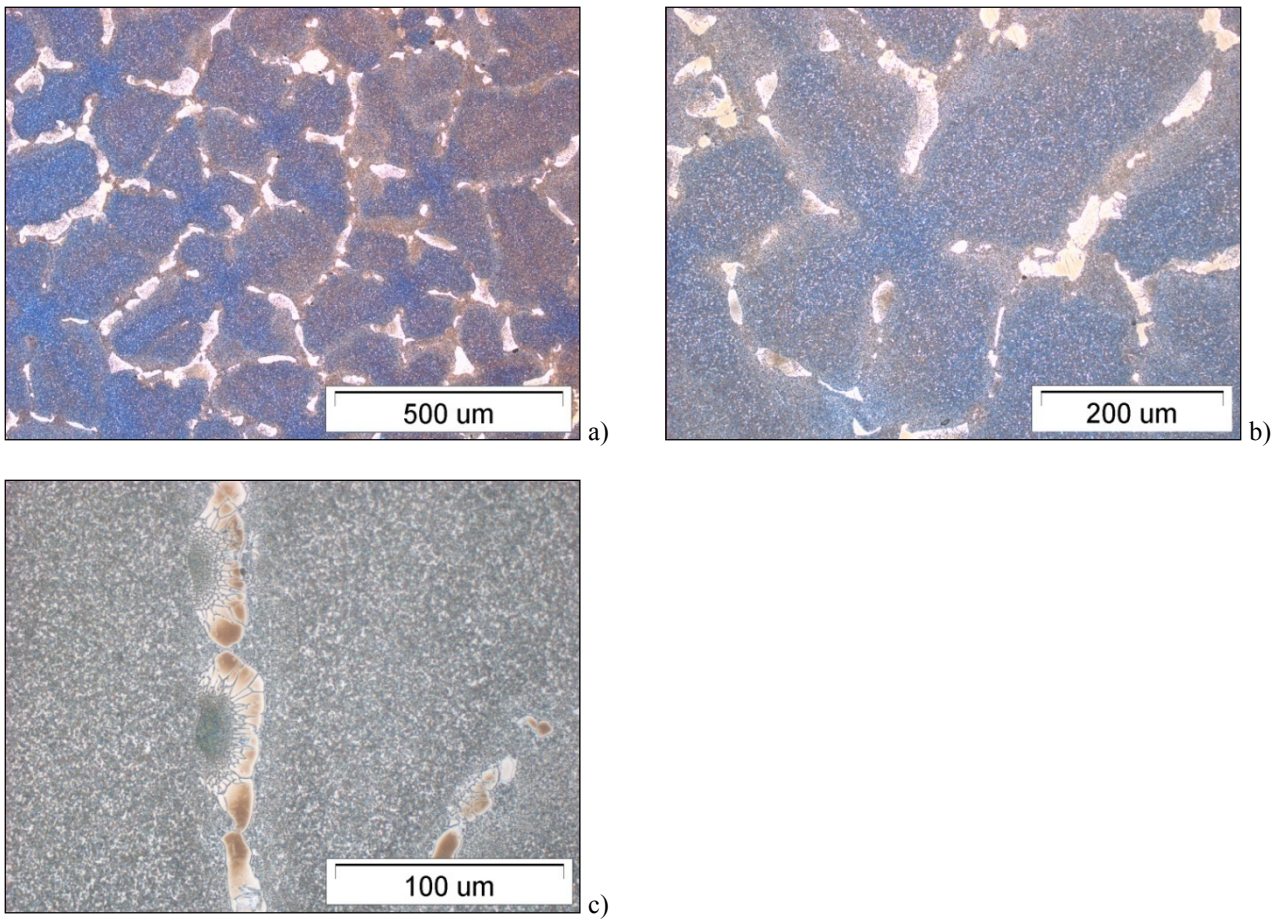

Fig. 1. Microstructure of CMSX-6 SC superalloy with application of various magnifications. LM, bright field (BF)

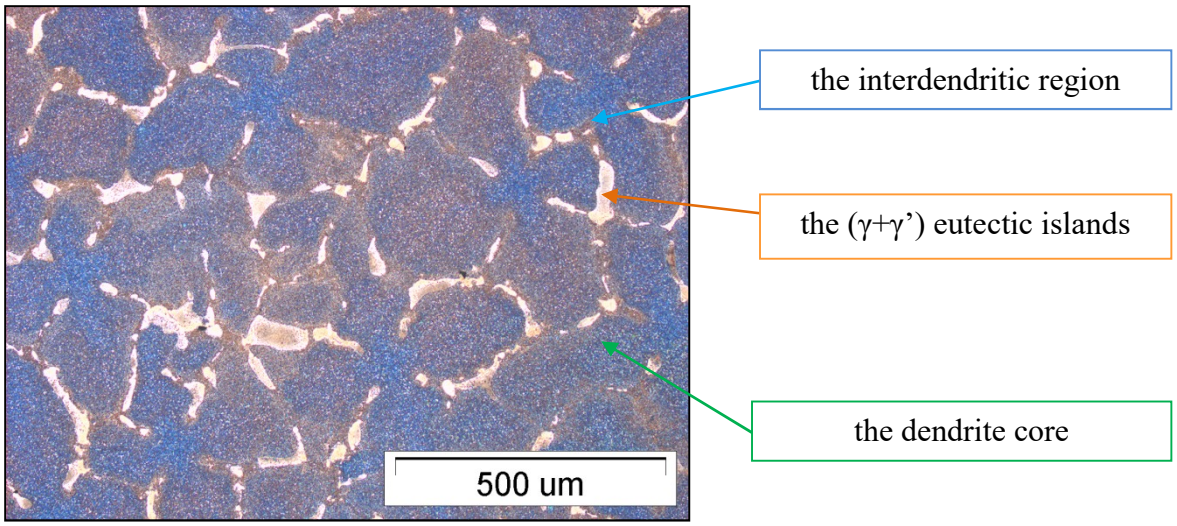

Fig. 2. Microstructure of CMSX-6 SC superalloy with marked three types of areas unlike each other. LM, BF

eutectic islands (the example of these regions detection on the same image as in Fig. 4 is shown in Fig. 5).

The author applied for the evaluation of the total volume fraction of the γ′ phase in the studied CMSX-6 superalloy the following formula proposed for other superalloy in Ref. [8]:

$$A_{A(\gamma')} = [A_{AD(\gamma')}*(A-A_E-A_{OE})+ A_{AE(\gamma')}*A_E+ A_{AOE(\gamma')}*A_{OE}] / A$$

where: $A_{A(\gamma')}$ – the total volume fraction of γ′ phase calculated; $A_{AD(\gamma')}$ – the area fraction of primary γ' phase measured at the dendritic cores; $A_{AE(\gamma')}$ – the area fraction of primary γ′ phase measured within the γ + γ′ eutectic islands; $A_{AOE(\gamma')}$ – the area fraction of primary γ' phase measured within interdendritic regions; A – the total area of measurement; A_E – the area of γ + γ. eutectic islands; A_{OE} – the area of interdendritic regions.

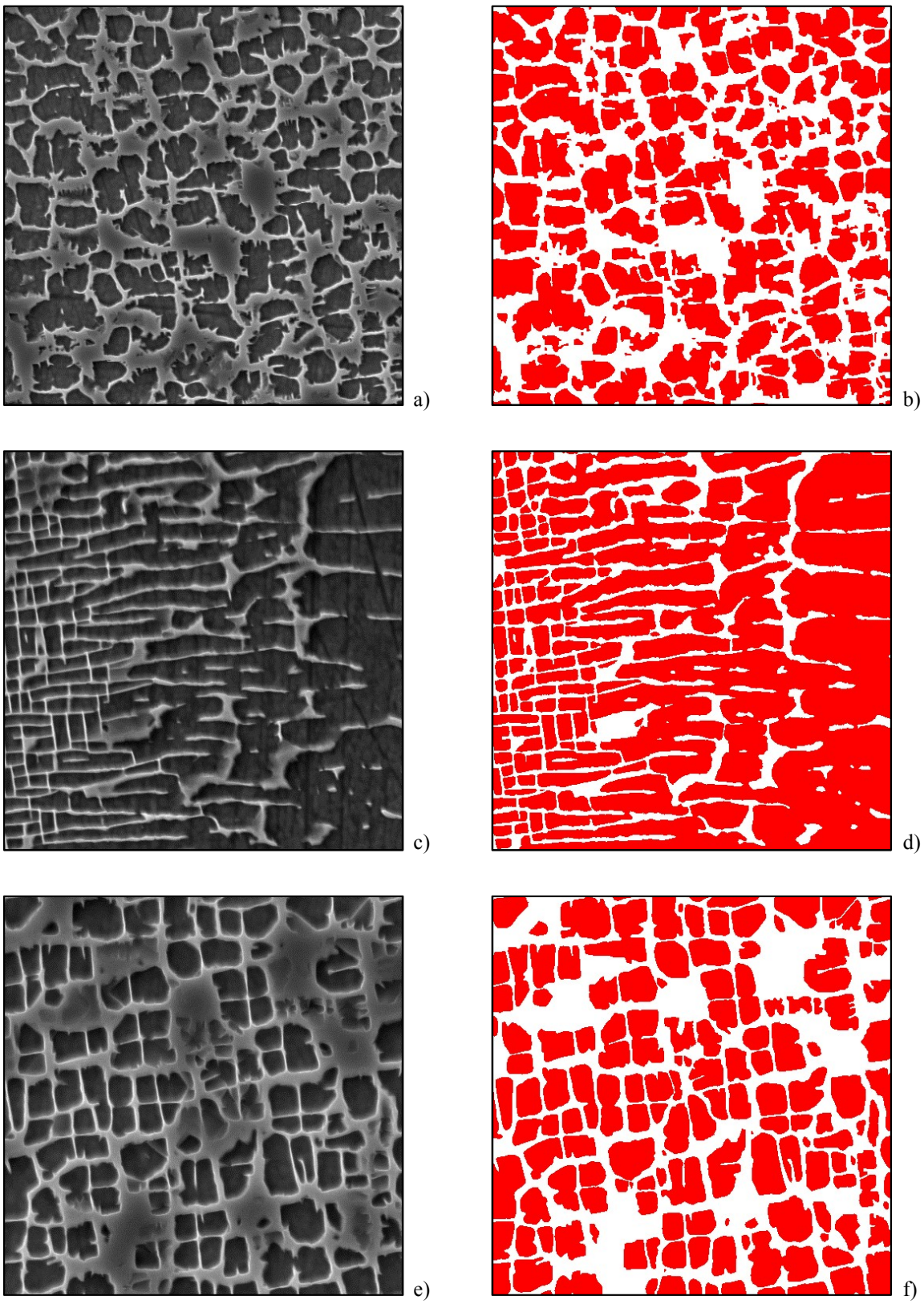

Fig. 3. Selected examples of detection of the γ' phase precipitates with differentiated morphology: a, b) the γ' phase precipitates at the interdendritic region; c, d) the γ' phase precipitates in ($\gamma + \gamma'$) eutectic; e, f) the γ' phase precipitates at the dendrite core

For the results obtained during the measurements the formula yields: $A_{A(\gamma')} = 0.59$, which means that the total calculated volume fraction of the γ' phase precipitates occurring in the investigated CMSX-6 superalloy amounts to 59.0%. The studied material was in as-cast state, that is why the presented result does not include a fraction of the finest γ' phase precipitates which can appear after heat treatment process and in this case the higher magnification and equipment is required for the volume fraction of the γ' phase precipitates calculation.

TABLE 3

The result of quantitative evaluation of the γ' phase precipitates occurring at the dendritic cores

Measured and estimated parameter	Result
area fraction of γ' phase precipitates A_A (γ'_1) [%] (A_A is an estimator of V_V)	59.44
mean area of γ' phase precipitate plane sections $\overline{A}$ [μm^2]	0.25
coefficient of variation of area of γ' phase precipitate plane sections $v(\overline{A})$ [%]	78.04
non-dimensional γ' phase precipitate shape factor $\overline{\xi} = 4*\pi*$area/(perimeter)^2 (mean value)	0.77
coefficient of variation of γ' phase precipitate shape factor $v(\xi)$ [%]	23.05
number of γ' phase precipitates per unit area of plane section N_A [mm^{-2}]	2451890.34
relative specific surface of γ' phase precipitates Sv/Vv [mm^2/mm^3]	9961.35
error of measurement of plane section area of γ' phase precipitates δ	0.04

TABLE 4

The result of quantitative evaluation of the γ' phase precipitates occurring within the ($\gamma + \gamma'$) eutectic islands

Measured and estimated parameter	Result
area fraction of γ' phase precipitates A_A (γ'_1) [%]	80.22
mean area of γ' phase precipitate plane sections $\overline{A}$ [μm^2]	0.64
coefficient of variation of area of γ' phase precipitate plane sections $v(\overline{A})$ [%]	891.10
non-dimensional γ' phase precipitate shape factor $\overline{\xi} = 4* \pi *$area/(perimeter)^2 (mean value)	0.81
coefficient of variation of γ' phase precipitate shape factor $v(\xi)$ [%]	29.35
number of γ' phase precipitates per unit area of plane section N_A [mm^{-2}]	1258321.20
relative specific surface of γ' phase precipitates Sv/Vv [mm^2/mm^3]	5742.75
error of measurement of plane section area of γ' phase precipitates δ	0.36

TABLE 5

The result of quantitative evaluation of the γ' phase precipitates occurring at the interdendritic regions

Measured and estimated parameter	Result
area fraction of γ' phase precipitates A_A (γ'_1) [%]	59.68
mean area of γ' phase precipitate plane sections $\overline{A}$ [μm^2]	0.62
coefficient of variation of area of γ' phase precipitate plane sections $v(\overline{A})$ [%]	143.30
non-dimensional γ' phase precipitate shape factor $\overline{\xi} = 4* \pi *$area/(perimeter)^2 (mean value)	0.70
coefficient of variation of γ' phase precipitate shape factor $v(\xi)$ [%]	36.42
number of γ' phase precipitates per unit area of plane section N_A [mm^{-2}]	970068.28
relative specific surface of γ' phase precipitates Sv/Vv [mm^2/mm^3]	6728.74
error of measurement of plane section area of γ' phase precipitates δ	0.05

4. Discussion and conclusions

Two kinds of observation method (SEM and LM) and wide range of magnification for the total volume fraction of the γ' phase precipitates determination were applied in this study. All the γ' phase particles were quantified by image analysis.

The main aim of the metallographic analysis in this study was to describe the γ' phase playing an important role in influencing the properties and the structural component (($\gamma + \gamma'$) eutectic) occurring in the investigated material. Generally, in scientific works a description of the γ' phase in nickel-base superalloys is usually, even not in every work, limited to the information about a volume fraction of this phase without further data about method or error of this evaluation. While the detailed description of this phase is essential because the γ' precipitates in Ni-based superalloys should be of optimum size, shape and distribution in order to have the desired properties and resist microstructural changes during service at high temperatures.

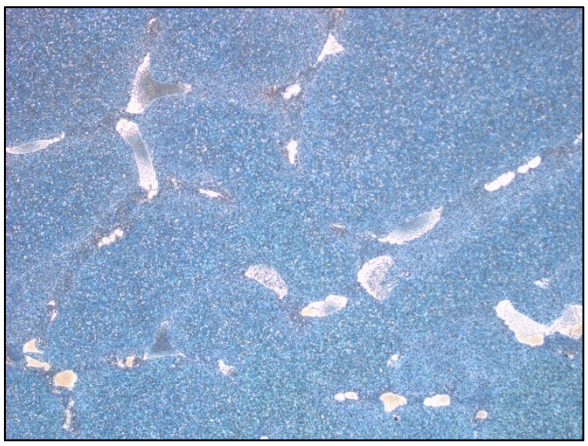

a)

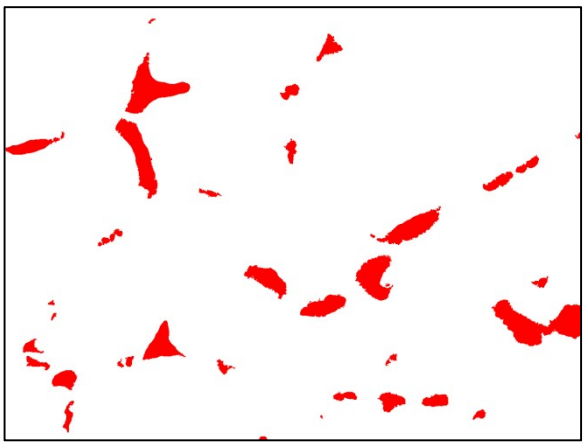

b)

Fig. 4. The example of detection of the ($\gamma + \gamma'$) eutectic islands: (a) initial image, LM, BF; (b) the detected areas of ($\gamma + \gamma'$) eutectic islands

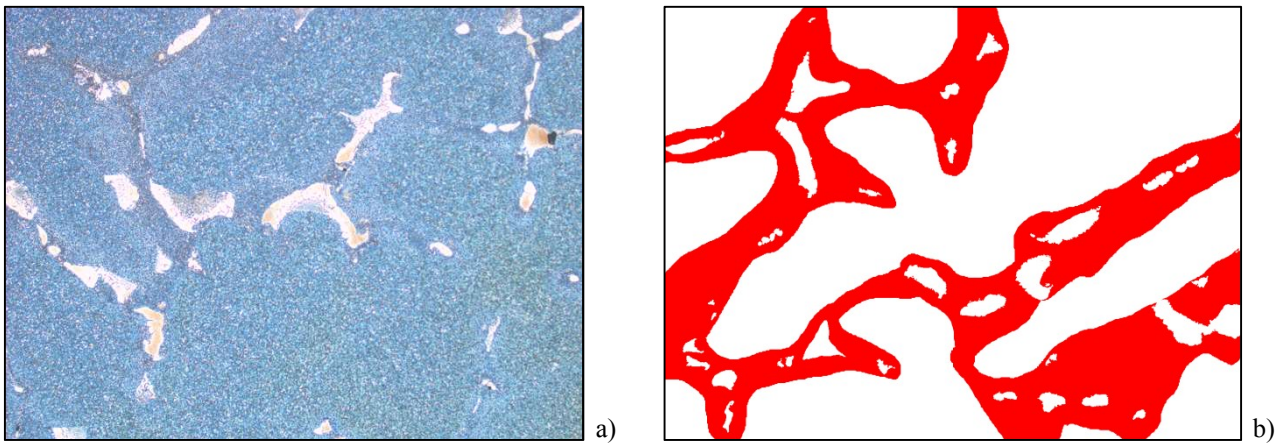

a) b)

Fig. 5. The example of detection of the interdendritic regions: (a) initial image, LM, BF; (b) the detected areas

A determination of the γ' phase volume fraction concerning the stereological characterization of the γ' phase in superalloys has been given in the several studies, e.g. [8-9]. In this study the formula including area of $(\gamma + \gamma')$ eutectic regions and interdendritic regions for the total area fraction of the γ' phase in the CMSX-6 superalloy has been applied. For the results obtained during the measurements using LM and SEM the total area fraction of the γ' phase precipitates occurring in the CMSX-6 superalloy investigated amounts to 59%. It is also essential to remember that this final value can be riddled with error of measurement of plane section area of γ' phase precipitates (δ in Tables 3-5). This error is the biggest in the case of the γ' phase particles within the $(\gamma + \gamma')$ eutectic areas, where the area fraction of the γ' phase precipitates (A_A), and mean area of the γ' phase precipitate plane sections ($\overline{A}$), and the coefficient of variation of area of the γ' phase precipitate plane sections $v(\overline{A})$ are the highest in comparison to dendrite cores and interdendritic areas. The mean value of a shape factor of the γ' phase precipitates is in the range from 0.7 (at the interdendritic areas) up to 0.81 (within $(\gamma + \gamma')$ eutectic islands). The number of γ' phase precipitates per unit area of plane section (N_A) is the lowest at the interdendritic areas, the higher within $(\gamma + \gamma')$ eutectic, and the highest in the dendrite cores. The opposite tendency you can observe taking into account a stereological parameter – relative specific surface of the γ' phase precipitates boundaries (S_V/V_v), which is characterized by the highest value in the case of the γ' phase precipitates occurring at the dendritic cores, the lowest value for the γ' phase precipitates within $(\gamma + \gamma')$ eutectic areas, and the middle value for the γ' phase precipitates at the interdendritic areas.

The γ' phase precipitates within $(\gamma + \gamma')$ eutectic areas and at the dendritic, and interdendritic areas vary in terms of their size and morphology. The visible dendritic structure and appearance and size of $(\gamma + \gamma')$ eutectic areas and the γ' phase precipitates pointed that heat treatment of this material is required.

The presented in this study results show similar value of the area fraction of the $(\gamma + \gamma')$ eutectic in CMSX-6 directionally solidified superalloy to that presented in Ref. [10]. The experimental results discussed in [11] show that the sizes of the eutectic pools decreased as the solidification rate increased. That is why presented in the study quantitative estimation of $(\gamma + \gamma')$ eutectic areas can be helpful during the investigations on the effect of technology process on a superalloy microstructure.

The obtainable in this study results confirm wide possibilities of modern software for computer facilities of research of metallography images with the aim of determination of quality and quantitative descriptions of engineering materials.

Acknowledgements

Financial support from the Structural Funds in the Operational Programme-Innovative Economy (IE OP) financed from the European Regional Fund-Project No POIG.0101.02-00-015/08 is gratefully acknowledged.

REFERENCES

[1] D.C. Zipperian, Metallographic Handbook, PACE Technologies, Tucson, Arizona, USA, 2011.

[2] Cannon-Muskegon Corporation. Alloy index. Muskegon, USA. 3rd edition, 2007.

[3] L. di Masso, B. Coluzzi, F.M. Mazzolaj, J. Phys. IV France **06**, C8-247-C8-250 (1996).

[4] J. Wortmann, R. Wege, G. Harris, G.L. Erickson, R.E. Schwer, Low Density Single Crystal Superalloy CMSX-6, 7th World Conference on Investment Casing, Munich, 1981.

[5] D. Ma, M. Meyer ter Vehn, P. Busse, P. Sahm, J. Phys. IV France, **03 C7**, C7-339-C7-342 (1993).

[6] Buehler Ltd. Buehler's Guide to Materials Preparation. The Argus Press, Niles, Illinois, USA, 2002.

[7] J. Szala, J. Cwajna, Acta Stereol. 18/1, 89-94 (1999).

[8] A. Szczotok, Materialwissensch. Werkstoffech. **46** (4/5), 320-329 (2015).

[9] A. Szczotok, J. Cwajna, Microsc. Microanal. **21** (3), 1339-1340 (2015).

[10] X. Li, J. Wang, J. Zhang, Y. Han, Xi Li, Materials **8**, 3428-3441 (2015).

[11] S. Zheng, Y.L. Jia, J. Tang, Mater. Sci. Forum **788**, 554-559 (2014).